

Time evolution of predictability of epidemics on networks

Petter Holme^{1,2,3,*} and Taro Takaguchi^{4,5}

¹*Department of Energy Science, Sungkyunkwan University, Suwon 440–746, Korea*

²*Department of Physics, Umeå University, 90187 Umeå, Sweden*

³*Department of Sociology, Stockholm University, 10961 Stockholm, Sweden*

⁴*National Institute of Informatics, 2-1-2 Hitotsubashi, Chiyoda-ku, Tokyo, 101-8430, Japan*

⁵*JST, ERATO, Kawarabayashi Large Graph Project, 2-1-2 Hitotsubashi, Chiyoda-ku, Tokyo, 101-8430, Japan*

Epidemic outbreaks of new pathogens, or known pathogens in new populations, spread fear much because they are hard to predict. For theoretical models of disease spreading, on the other hand, quantities characterizing the outbreak converge to deterministic functions of time. Our goal in this paper is to shed some light on this apparent discrepancy. We measure the diversity of (and, thus, the predictability of) outbreak sizes and extinction times as functions of time given different scenarios of the amount of information available. Under the assumption of perfect information—i.e. knowing the state of each individual with respect to the disease—the predictability decreases exponentially, or faster, with time. The decay is slowest for intermediate values of the per-contact transmission probability. With a weaker assumption on the information available, assuming that we know only the fraction of currently infectious, recovered or susceptible individuals, the predictability also decreases exponentially most of the time. There are, however, some peculiar regions in this scenario where the predictability decreases. In other words, to predict its final size with a given accuracy, we would need increasingly much information about the outbreak.

PACS numbers: 64.60.aq,89.65.-s,87.23.Cc

I. INTRODUCTION

Outbreaks of serious infectious diseases have an ability to scare people even though they many times die out before they reach the worrying person. Part of the reason for this is that it is hard to forecast disease outbreaks (see e.g. Refs. [1, 2]), and this uncertainty adds to the scare. At the same time, our common models for disease spreading behave, once they taken hold in the population [3], like deterministic, perfectly predictable, quantities [4]. Such models have two components. First, they model the person-to-person contagion and the history one individual with respect to the disease. This is done by dividing individuals into states (or “compartments”) with respect to the disease, and assigning rules for transitions between the states. A canonical model of diseases that make the infectious person immune upon recovery (or kill their host) is the Susceptible-Infectious-Recovered (SIR) model. This model has three classes: susceptible individuals can acquire the disease, infectious individuals can spread it further, and recovered (who technically speaking also can be dead) cannot get, and do not spread the disease. The transition rules are that a susceptible, upon meeting an infectious, can (with some probability) become infectious, and after some time, or with some probability, recovers or dies. These transitions are assumed to be instantaneous (which is a quite coarse simplification with respect to real diseases). The second component of epidemic models describes the population level processes over which the pathogen propagate. For decades, theoretical epidemiologists have ignored this issue and taken the “well-mixed assumption”—that any pair of individuals have the same chance of meeting during an interval of time. Re-

cently researchers have recognized this problem and represented the contact structure as a network [5–7]. The regularities, or *structure*, of the network have a great impact on the evolution of disease outbreaks. Among the network structures, the one with strongest influence is perhaps the degree distribution—the probability distribution of the number of neighbors. This structure have explained the existence of super-spreaders [8] and challenged the existence of an epidemic threshold below which an outbreak would always die out quickly [18]. Now, if one studies the SIR process on the configuration model [9]—random networks with an arbitrary degree distribution—the outbreak turns out to be completely predictable in the long-time and large- N limits [4]. To be specific, population-averaged quantities such as the fraction of infected individuals converge to deterministic functions of time. The major uncertainty is in the very beginning, whether the outbreak would die out immediately or not. There is thus an apparent contradiction—our canonical compartmental models seem unable to capture the uncertainty of real world outbreaks.

In this work, we investigate how the predictability of SIR processes evolves with the outbreak itself. We study questions such as: Assuming an outbreak started some time t ago, then what can we say about the final number of infected people Ω and the extinction time τ as a function of t ? How does our ability to predict Ω and τ depend on the network structure and the type of information we have about the outbreak?

II. PRELIMINARIES

In this section, we will clarify the methods and precise model definitions in the rest of the paper. We also mention some computational considerations.

*Electronic address: holme@skku.edu

A. SIR simulation

We assume there is a disease spreading over a static underlying network represented as a graph $G = (V, E)$. V is a set of vertices representing individuals of the population; E is a set of edges representing (unordered) pairs of individuals in close enough contact for the disease to spread. The number of vertices is denoted N and the number of edges M . The vertices are, at a given time, in one of three states—S (meaning that they do not have the disease, but they can get it), I (meaning that they have the disease and they can spread it) and R (meaning that they do not have the disease and they cannot get it). We assume a disease outbreak starts at $t = 0$. At the beginning all vertices belong to the state S, except a randomly chosen vertex that is in state I. If a pair $(i, j) \in E$ consists of one I and one S vertex, then the S vertex has a chance β of becoming I (otherwise it stays S). We call this an *infection event*. Every vertex with state I has a chance ν per time unit of becoming R (in a *recovery event*). The state of the system at a certain time could thus be fully described by two vectors: $\mathbf{s} = (s_1, \dots, s_N)$ giving the state of each vertex ($s_i \in \{S, I, R\}$) and a vector $\mathbf{t}_I = (t_1^I, \dots, t_N^I)$ giving the infection time of the vertices.

Most important quantities describing the outbreak will only depend on the ratio between β and ν (in the well-mixed SIR model this ratio is called R_0 , but to not confuse things, we do not use this name). The actual values of β and ν are only needed to calculate the real time to reach the peak prevalence, extinction, etc. That does not interest us in the present paper, so we measure time in units of $1/\nu$. In a simulation, this can conveniently be done by (at an iteration of the algorithm) performing a random infection event with a probability

$$P = \frac{\beta \Sigma}{\beta \Sigma + I} \quad (1)$$

where Σ is the number of edges between an I and an S vertex, and I is the prevalence (note that roman letters symbolize a state and italicized letters represent the number of vertices in the corresponding state) [10]. The factor $\Delta t = (\beta \Sigma + I)^{-1}$ represents the time increment since the last iteration. Thus, to keep track of the time (in units of $1/\nu$) one adds Δt to a variable representing time. If an infection event is not performed (which happens with a probability $1 - P$), we perform a recovery event. In an infection event, the SI edge (to become II) is chosen randomly among all SI edges. Similarly, in a recovery event, the I vertex (to become R) is selected with uniform randomness among all I vertices.

B. Network models

To study the effects of network topology on the outbreak predictability, we use a collection of six network models. We chose the models to reflect a variety of stylized network topologies. This methodology is inspired by Ref. [11]. Throughout this paper, we will use graphs of size $N = 2500$. We use 1,000 realizations of each network model. A summary

of the basic network structure in these networks can be found in Table I.

1. Large- and small-world networks

First, we use the Watts-Strogatz small-world network model [12]. In this model, all vertices have the same degree k (number of neighbors). They are initially arranged on a ring and connected to their $k/2$ nearest neighbors, at either side, of the ring. Counting modulo N , these neighbors can be enumerated as $i - k/2, i - k/2 + 1, \dots, i - 1, i + 1, \dots, i + k/2$. Then one goes through all vertices i around the ring, and for every edge (i, j) pointing to a neighbor ahead (i.e. $j > i$ modulo N), with a probability p replaces (or “rewires”) it by (i, j') (where j' is a different vertex from i and $(i, j') \notin E$). By construction, if $p = 0$ and $k > 2$, this model gives networks with a high density of triangles. Furthermore, for these parameter values, the average distances grows like N . Watts and Strogatz show that if p is slightly larger than zero, the distances scales much slower with N . The number of triangles is, on the other hand, not so sensitive to p . The reason for this behavior, is that the rewired edges (usually called “long-range edges”, with reference to the ring topology) connects distance parts of the graph. For the triangles, only the directly involved vertices are affected by a rewiring, but for the distances the extended neighborhoods of these vertices are affected. In this work, we use the Watts-Strogatz model with $p = 0$ (calling it *large-world networks*) and $p = 0.01$ (calling it *small-world networks*). We use $M = 5,000$, so the small world networks have an expected number of 50 rewired edges. The large-world networks, of course, are all isomorphic and only one copy of them is needed as a substrate for our simulations.

2. Random regular graphs

Random regular graphs [13] are designed to be as uniform as possible with respect to the positions of vertices. Like the Watts-Strogatz model, all vertices have the same degree $k = 4$ (giving $M = 5,000$). Other than that, they are as random as possible. In graph models with less restrictions (like Erdős-Rényi random graphs [14] where there is a fixed probability for any vertex pair to belong to E) the degrees vary, which differentiates the vertices. On the other hand, for our purpose, Erdős-Rényi graphs would probably give very similar results.

3. Scale-free networks

So far, all the model networks we discussed have uniform degree distributions. This is not very realistic. Rather, the degrees of empirical networks are in general often broadly and skewedly distributed. This is also true for the some of the particular networks diseases spread over, like sexual networks [15] or networks of contacts between patients in hospitals [16]. To model such networks, we use the configuration

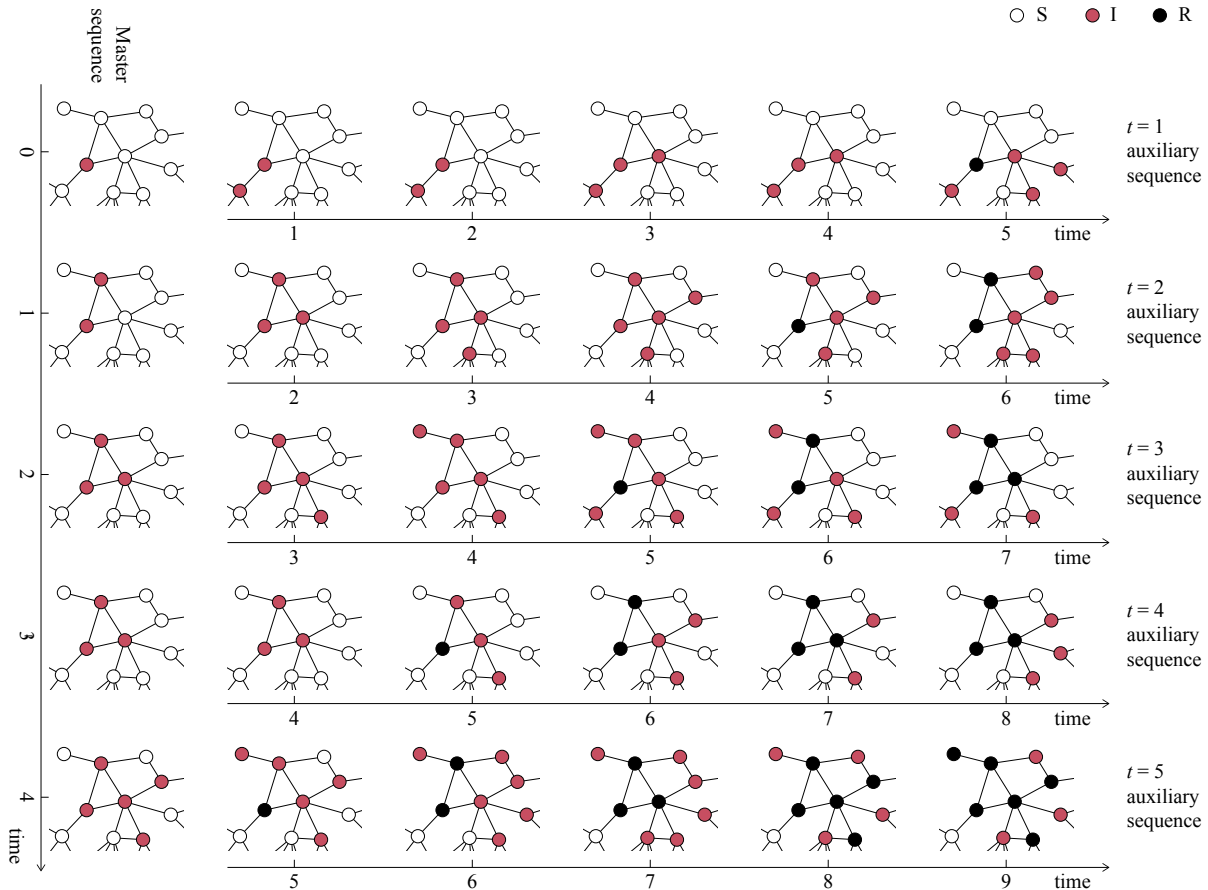


FIG. 1: (Color online) Illustration of the methodology to study the decay of predictability in the case of maximal information of the system. First we run a master sequence simulation of the SIR process on a network. At every time step, we break this simulation and use the configuration as a seed for 1,000 auxiliary simulations. The standard deviation of the final outbreak size and time to extinction thus captures how accurately the outbreak can be predicted given the state of the system at the breaking point.

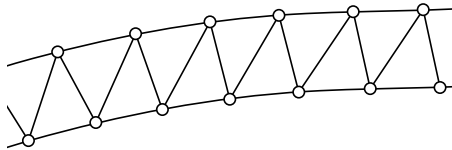


FIG. 2: The local structure of the Watts-Strogatz model networks with $k = 4$.

model [14] with an emerging power-law degree distribution. We draw N integers $\{k_i\}_{i=1}^N$ from a probability distribution

$$P(k) = \begin{cases} k^{-\gamma} & \text{if } 1 \leq k \leq N-1 \\ 0 & \text{otherwise} \end{cases} \quad (2)$$

until $\sum_{i=1}^N k_i$ is even. Then we randomly attach edges between vertices until vertex i has k_i neighbors. We do not forbid multiple edges or self-edges. I.e., the resulting object is a multigraph. The upper limit $N-1$ is somewhat arbitrarily chosen to be the same as the maximum degree in a simple graph. This is needed to keep the fluctuations down (that comes from the extreme variation if k generated by small γ values). Finally,

we construct a simple graph by removing multiple edges and self-edges. We try three different γ values from the typical range of empirical networks [17]: 2, 2.5 and 3.

4. Theoretical threshold values

As mentioned, an interesting feature of epidemic models is that they can have a threshold behavior where the average fraction of infected individuals is finite as $N \rightarrow \infty$ provided that β is larger than a threshold value β_c . By analogy to models in statistical physics, this could be described as a continuous phase transition [7]. This is not the focus of our study, but we will review a few theoretical results for our models to give some context.

The large-world and scale-free networks have thresholds for the extreme values of β . In the large-world network case, the epidemics spread along a one-dimensional chain (Fig. 2). For any $\beta < 1$ value there is a finite chance that the outbreak will stop, so there is an expected distance it will propagate from the seed. The outbreaks are limited by this finite distance, so if $N \rightarrow \infty$ the fraction of affected vertices is zero.

TABLE I: Summarizing the network structure of the six classes of networks we study. All networks have 2,000 vertices. Except the large-world network (which is unique), we use the same 1,000 independent realizations as in the rest of the work. In the second row we list the standard deviation (once again with the exception for the large-world network).

network model	M	s	d	C
large world	5,000	1	312.8	0.5
small world	5,000	1	36.6	0.484
	0	0	3.69	0.00236
random regular	5,000	1	6.47	0.000964
	0	0	0.00401	0.000440
scale free, $\gamma = 2$	6696	0.963	3.24	0.0666
	365	0.00783	0.125	0.0132
scale free, $\gamma = 2.5$	3039	0.785	4.54	0.0153
	160	0.0271	0.464	0.00497
scale free, $\gamma = 3$	2046	0.46	6.88	0.00277
	69.3	0.0459	1.01	0.00161

For the scale-free networks of the exponents that we study, the threshold is $\beta_c = 0$ [7, 18]. The random regular networks have a threshold $\beta_c = 1$ [7]. The small-world networks in the limit $p = 1$ have $\beta_c = 2/7$ [19], but we are not aware of any derivations of the threshold for $0 < p < 1$.

III. PREDICTABILITY GIVEN THE STATE OF THE SYSTEM

The predictability of any kind of phenomenon depends on the information available and the ability to use it. In this paper, we assume that the disease spreading is determined by the SIR process. Assume we know the precise state of the system—the underlying network, the state of all vertices and when they changed state. In that case one cannot, by definition, do better in predicting the future than evaluating the SIR process with the state of the system as the input. In this section, we focus on this limit of maximum information about an outbreak.

A. Methods

We want to understand how the predictability of Ω and τ depends on t given that we know \mathbf{s} and \mathbf{t}^\dagger . To this end, we run an SIR simulation producing a *master sequence* $(\mathbf{s}_0, \mathbf{t}_0^\dagger)$ and at every time step, we start 1,000 simulation runs with $(\mathbf{s}_0, \mathbf{t}_0^\dagger)$ as the initial condition. The standard deviations of Ω and τ of these *auxiliary sequences* measures the unpredictability evolution of the master sequence. Finally, we average these standard deviations over at least 2,000 master sequences and call them σ_Ω (for the outbreak size) and σ_τ (for the extinction time). For each such sequence, we take a random network realization from a pool of 1,000. When an outbreak is dead (when $\Sigma = 0$), it contributes with a standard deviation of zero to the average. This procedure is illustrated in Fig. 1.

B. Results

Now we will turn to our numerical results relating to the predictability. Statistics about the outbreak durations, average prevalence and average number of susceptible vertices can be found in the Supplementary material.

1. Predicting the final outbreak size

We start by investigating the σ_Ω for our six classes of networks for an exponentially increasing sequence of 11 β values. We chose the β values so that we cover outbreaks of all sizes, in all network models. We plot the results in Fig. 3. Our first observation is that none of the curves (i.e. for no β value and for no topology) decays slower than exponential. Most of them decay roughly exponentially, while some decay more rapidly. The faster-than-exponential decay is clearest for the highest β curves of the small- and large-world networks (see Figs. 3(a) and (b)). The random-regular graphs in Fig. 3(c) do not have the same fast drop-off. Since all three models in Figs. 3(a)–(c) have uniform degree distribution, the explanation must be something else. Locally, the large- and small-world networks look the same—bands of stacked triangles (see Fig. 2). We believe the cut-off of the exponential decay relate to the typical length of these bands. So for example, the $\beta = 8$ curve in Fig. 2(b) bends down around $t = 32$. Our interpretation is that the early, slower decay is a period where none of the outbreaks have reached the entire population. For the other models, since the outbreak can reach the entire population much faster, these two regions get blurred and the result is just one exponential decay. Comparing curves of different β , we see that the ones with slowest decay are the ones with the longest extinction times. Presumably, as an extinct outbreak is perfectly predictable, the extinction time is an important factor in determining the time evolution of predictability. This would explain why intermediate β values have the slowest decay of predictability—extinction times will initially grow with β (as the chance for an early extinction decreases), then decrease (because the increasingly fast spread and subsequent burn-out in the population [20]). This is however not the case for the scale-free networks in the same parameter range. In Figs. 3(d)–(f), we plot the results for scale-free networks. For $\gamma = 2.5$ and 3, when β is small, T is almost constant. σ_Ω still increases with β , but this increase happens in the early die-off (mentioned in the Introduction). In other words, smaller β affects σ_Ω by increasing the chance of the disease to die in the very early stage. Once the outbreak gets a hold in the population, the predictability decays independent of β . For larger β , over the peak in extinction time, the lifetime decreases with β .

To investigate the relationship between the decay of σ_Ω and β closer, we assume the scaling form $\sigma_\Omega \sim \exp(-t/T)$ and measure T [21]. Note that this assumption is not justified by any rigorous theory—it should be regarded as a somewhat sketchy summary of Fig. 3. In Fig. 4, we show the results. Some of the curves (as mentioned) do not have an exponential tail and are excluded from this analysis. This figure illustrates how, except maybe the $\gamma = 2$ scale-free network, all curves of

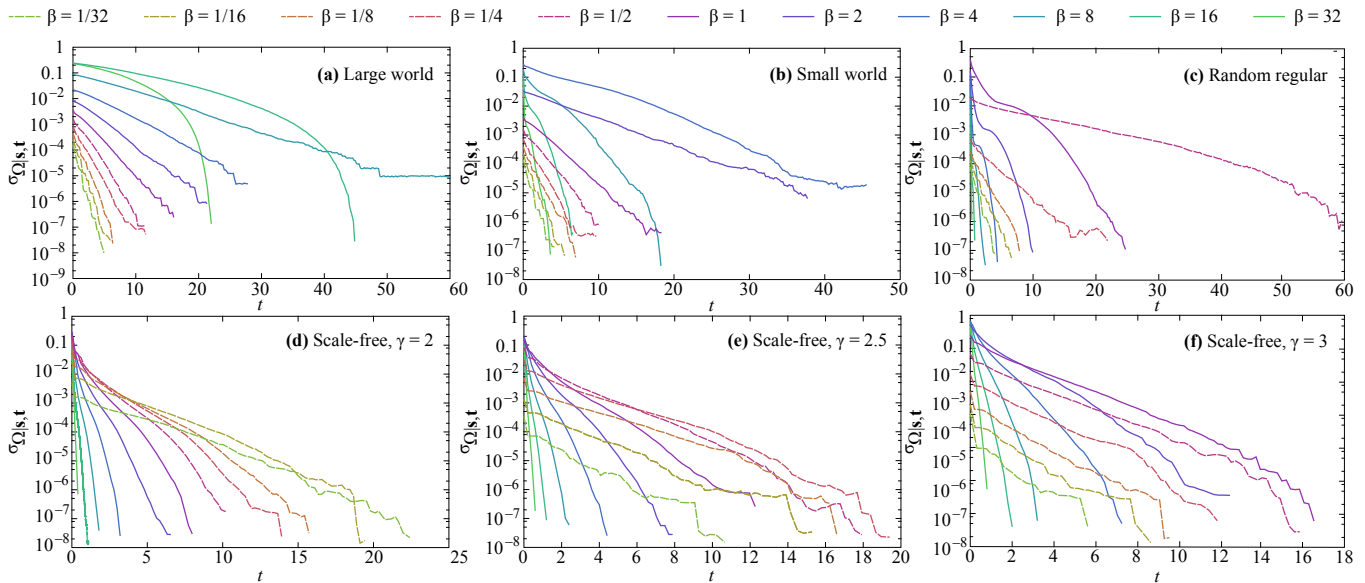


FIG. 3: (Color online) We show the standard deviation of the final outbreak size given the state at t as a function of t . As σ_Ω measures the outbreak diversity, its increase reflects the decay of predictability. The curves ends when the all the simulated outbreaks have died. In principle σ_Ω is defined for any $t > 0$, but after the outbreaks are over it is zero and thus not visible in this figure.

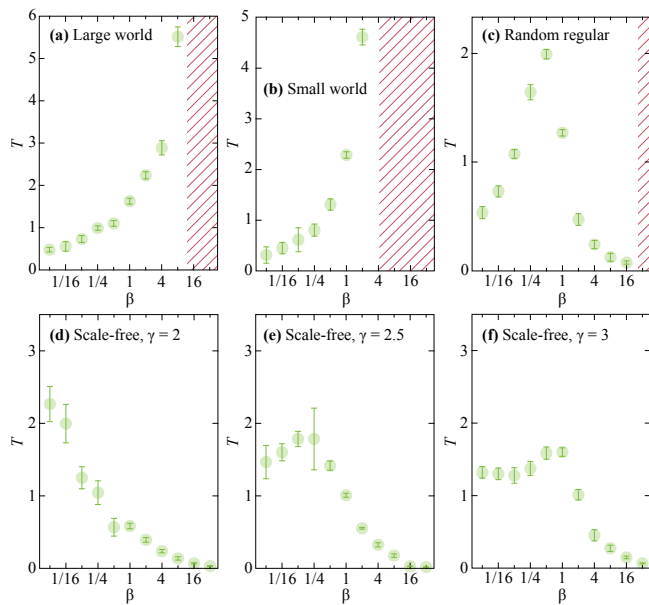


FIG. 4: (Color online) The decay constants from non-linear least-squares fits to exponential forms of the curves in Fig. 3. The shaded regions indicate where the σ_Ω does not fit an exponential function.

Fig. 3 have the slowest decay of σ_Ω for intermediate β values. It seems reasonable that the location of this peak converges to the epidemic threshold as $N \rightarrow \infty$. On the other hand, none of the Fig. 3 curves have a concave shape indicative of a slower-than exponential decay (which one could expect if σ_Ω was a critical parameter, diverging at the threshold). An alternative hypothesis is that this peak coincides with the maximal extinction time, which is thought to be larger than, but distinct from,

the epidemic threshold [20]. We will leave this as a question for future studies.

2. Predicting the extinction time

In addition to studying the (un)predictability with respect to outbreak size, we also study σ_τ —the corresponding quantity for the extinction time τ —in Fig. 5. The general picture from Fig. 3 holds—the decay is roughly exponential. However, there is more structure in these curves. The decay fits the exponential form worse than what σ_Ω does. Several of the σ_τ curves for the random-regular and scale-free graphs plateau at intermediate β values. This means there are times where predicting the outbreak size get more precise with time, but predicting how long the epidemics will last does not.

IV. PREDICTABILITY GIVEN THE SIZES OF COMPARTMENTS

In Sec. III, we studied the scenario where we have maximum information about an outbreak. This is of course an idealized situation, and in this section, we turn to the more realistic scenario where we know the number of people infected and recovered, but not who is in what state.

To assess the predictability based on the summarized information about the system, we redefine the measure of predictability σ_Ω by the standard deviation of Ω conditioned on the number of I vertices (I), R vertices (R), and I or R vertices. We denote the measures redefined as $\sigma_{\Omega|I}$, $\sigma_{\Omega|R}$, and $\sigma_{\Omega|I+R}$, respectively. Note that, because the total number of vertices is fixed to N , $\sigma_{\Omega|I+R}$ is equivalent to that conditioned

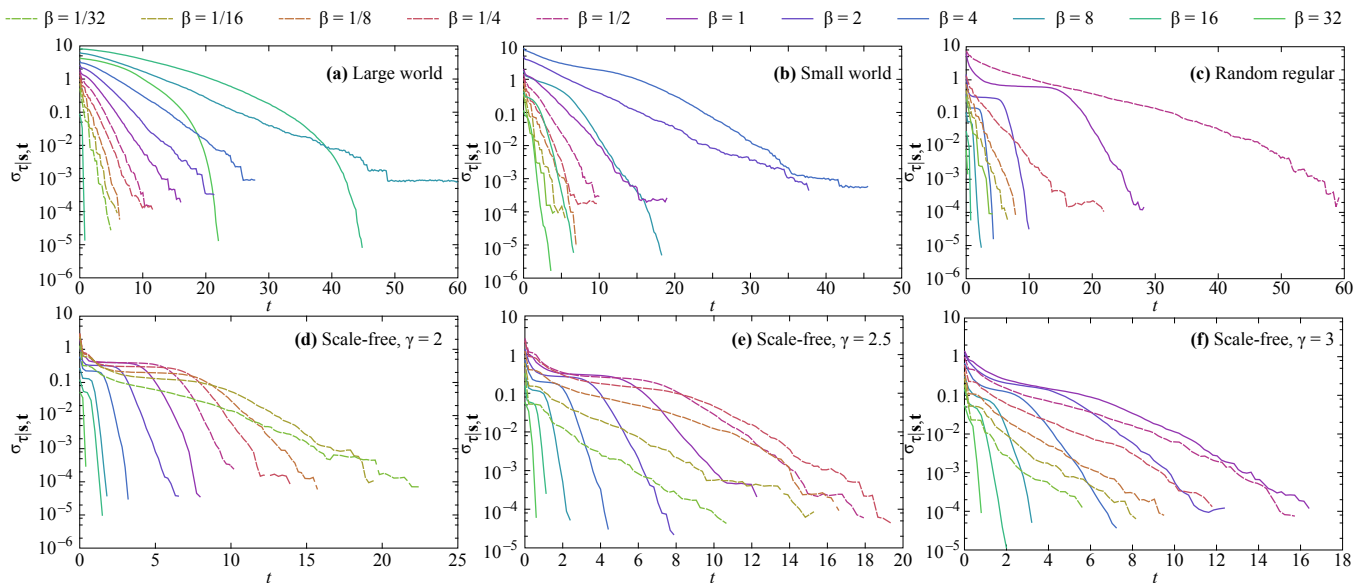


FIG. 5: (Color online) This figure corresponds to Fig. 3 but shows the standard deviation of the extinction time rather than the outbreak size.

on the number of S vertices. We calculate these measures as follows (we take $\sigma_{\Omega|I}$ as an example). Instead of setting a master sequence as we did in Sec. III, we first numerically simulate 10,000 runs with the initial seed chosen randomly on the given network realization. We pick out the runs with the same I value among the runs and calculate the standard deviation of Ω . Finally, we take average of this standard deviation over all I values (i.e., from 0 to N) and obtain $\sigma_{\Omega|I}$. For deriving $\sigma_{\Omega|R}$ and $\sigma_{\Omega|I+R}$, we perform the same calculation based on R and $I+R$.

The resultant predictability measures $\sigma_{\Omega|I}$, $\sigma_{\Omega|R}$, and $\sigma_{\Omega|I+R}$ are plotted as a function of time t in Figs. 6, 7, and 8, respectively. Note that we use the same set of network realizations that we used in Sec. III. It also should be noted that the range of extinction time shown in Figs. 6, 7, and 8 are larger than those shown in Figs. 3 and 5, simply because we consider a larger number of simulation runs than we did in Sec. III. To be precise, here we consider 10^7 simulation runs, i.e., 10^4 runs on each of 10^3 network realizations.

For all of the network models, we observe a bump in $\sigma_{\Omega|I}$ (see Fig. 6). When we increase the β value, we find the bump is located at the range of larger t up to a certain β value and is located closer to $t=0$ when we further increase β . In particular, for scale-free networks with $\gamma=2$, we observe that the bump is located at the largest t when $1/32$. The presence of a bump in the $\sigma_{\Omega|I}$ curves can be explained as follows. At the beginning of the process, $\sigma_{\Omega|I}$ decreases with time t because the standard deviation of Ω among the runs with the same I values gets smaller as the runs are separated into ones rapidly dying out and those eventually going outbreaks. In the middle term of the process, $\sigma_{\Omega|I}$ increases with time t because a number of runs, regardless of Ω , fall into the range of the small I values near extinction. In the end of the process, $\sigma_{\Omega|I}$ decreases with time t because all the runs die out and become perfectly predictable (as $I=0$). These observations suggest

that $\sigma_{\Omega|I}$ holds the prediction power at the early stage of the epidemic process; however, it becomes unreliable as a predictor at the late stage.

By contrast to the non-monotonical behavior of $\sigma_{\Omega|I}$, the other measures $\sigma_{\Omega|R}$ and $\sigma_{\Omega|I+R}$ are non-increasing functions with time except for the range of very small t (see Figs. 7 and 8). This implies that the predictability of the SIR processes increases with time if we know the R value (and the I value in addition). In particular, the $\sigma_{\Omega|I+R}$ curves exhibit the dependence on different β values which is very similar to the σ_{Ω} curves shown in Fig. 3. This observation is supported by the decay exponents of the $\sigma_{\Omega|I+R}$ curves fitted with an exponential form (Fig. 9), which indicate dependence on β similar to that of σ_{Ω} (see Fig. 4). In other words, once we have such a summarized value about the system's state, we can achieve the prediction power (in terms of $\sigma_{\Omega|I+R}$) as much as when we have the perfect information about the system, for the network models we consider.

V. SUMMARY AND DISCUSSION

In this paper, we numerically investigated the predictability of outbreaks of the SIR epidemic process on static network models. We used the standard deviation of the final outbreak sizes conditioned on the state of vertices at a given time as a key-quantity for predictability (technically speaking unpredictability, since zero standard deviation means that the outcome is perfectly predictable). We considered the two scenarios of the information available. First, that we have perfect information of the system (where we know the exact state of the vertices (\mathbf{s}, \mathbf{t}^1)). Second, that we have partial information—to be precise, only the number of infected I or recovered R . In the first scenario, the standard deviation $\sigma_{\Omega|s,t}$ decays like an exponential function of time, or slower, for all the types of

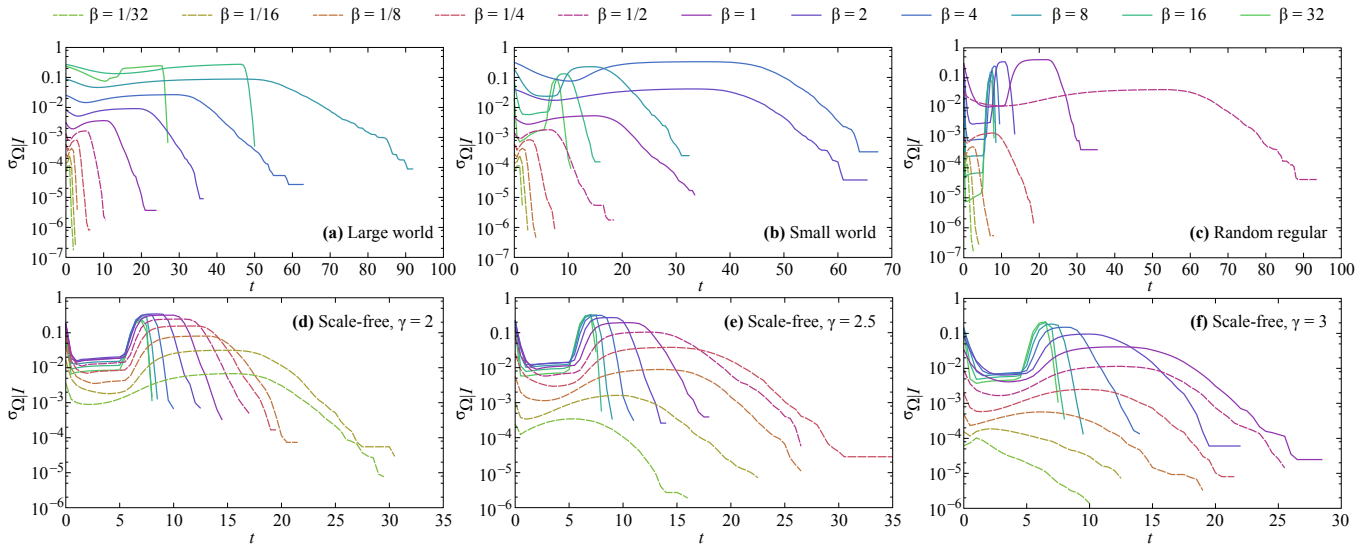


FIG. 6: (Color online) Standard deviation of the final outbreak sizes conditioned on I , that is, the number of infected vertices at t .

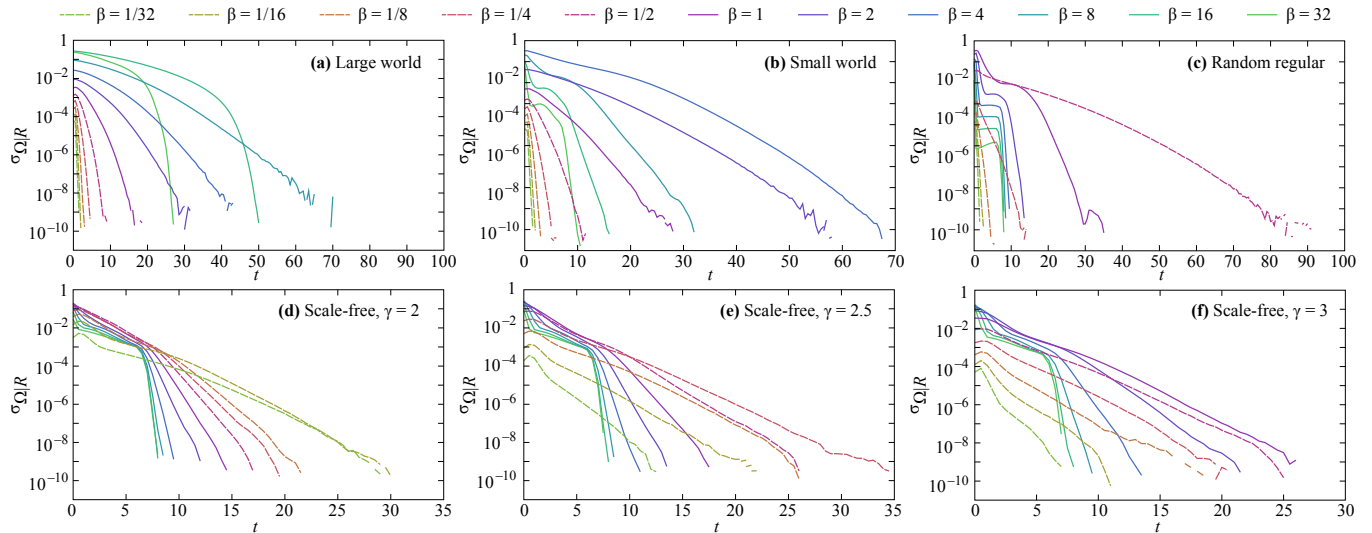


FIG. 7: (Color online) Standard deviation of the final outbreak sizes conditioned on R , that is, the number of recovered vertices at t .

network models we considered. This result is consistent with the previous theoretical result that the characteristic quantities of the SIR process asymptotically converges to deterministic functions [4]. The time constant of the exponential decay, however, is highly model dependent. We saw a monotonic increase of the decay exponent for the large- and small-world networks, whereas a monotonic decrease was observed for the scale-free networks with $\gamma = 2$. For the random regular graph and the scale-free networks with $\gamma = 2.5$ and 3 , there is a single peak of the decay exponent at an intermediate value of β . These results shed new light on the notion of predictability of SIR process, i.e., the uncertainty in epidemic outbreaks is a nontrivial question even if we possess the information of contact network structure and vertices' states.

For the second scenario, the standard deviation $\sigma_{\Omega|R}$ and $\sigma_{\Omega|I+R}$ decay with exponential tails, while $\sigma_{\Omega|I}$ exhibits non-

monotonic change in time. Specifically, for large transmission rates it has a peak for intermediate times. In other words, some time after the outbreak starts, we can expect that knowing e.g. the prevalence becomes less valuable. It is also in this region where there is a large difference between the two scenarios, i.e., knowing the exact configuration of infectious, susceptible and recovered improves the predictability much. Another way of seeing this is that for most parts of the parameter space, the additional information in our first scenario rarely of much use, still it is fairly much more information ($2N$ numbers as opposed to one number).

Connecting back to our starting point—how could real outbreaks be hard to predict when the SIR model itself converges to deterministic quantities—we see, as mentioned, that for some parameter values, assuming only aggregate information, the convergence is slow. A possible answer is that the discrep-

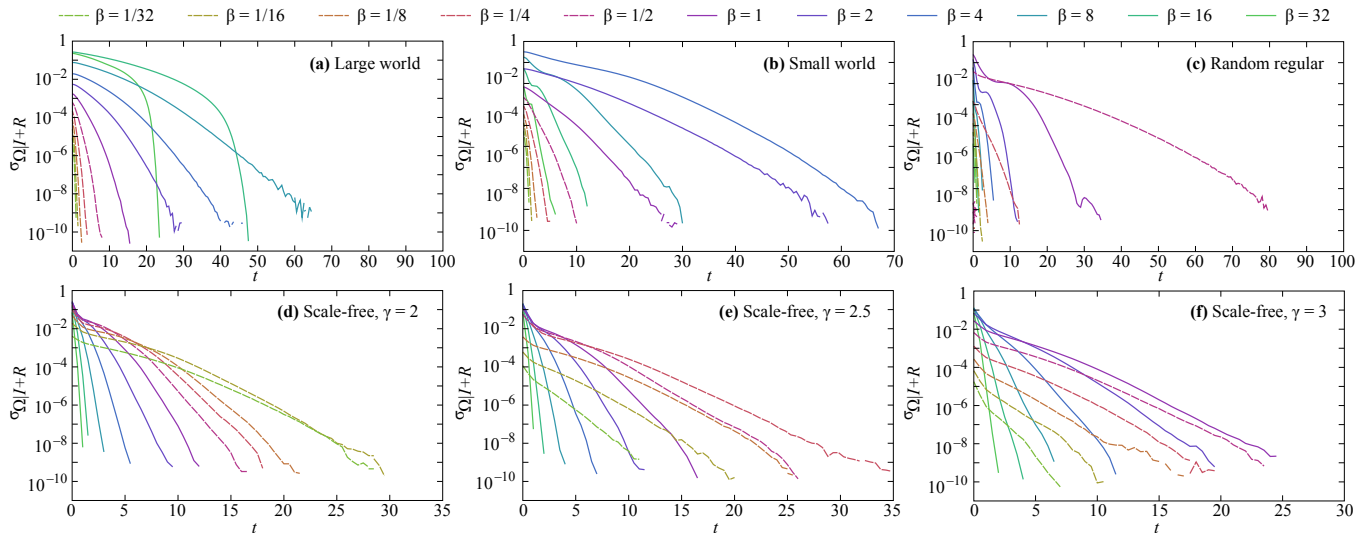


FIG. 8: (Color online) Standard deviation of the final outbreak sizes conditioned on $I+R$, that is, the number of infected and recovered vertices at t .

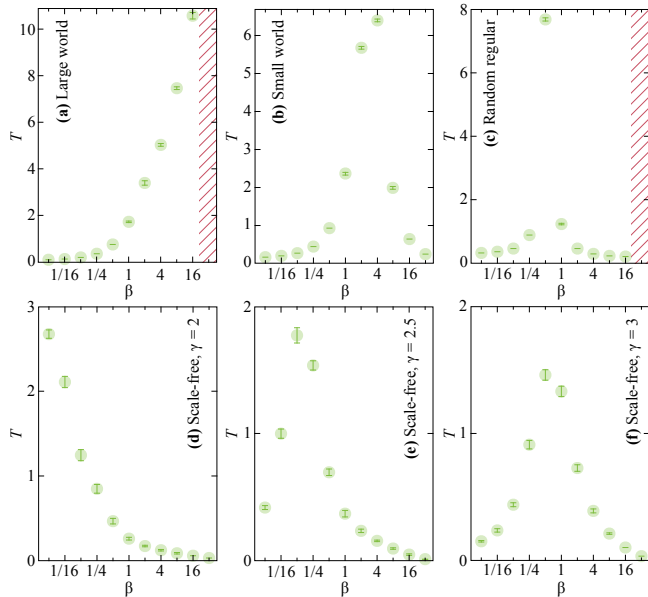


FIG. 9: (Color online) The decay constants from non-linear least-squares fits to exponential forms of the curves of $\sigma_{\Omega/I+R}$ shown in Fig. 8.

ancy comes from that we in practice only have this kind of aggregate information. On the other hand, for many parameter values, also in the case of population-level information, the decay of predictability is very fast (also compared to the duration of the outbreak). For this reason, we also believe that the SIR model (i.e., the assumptions behind it), to some extent, underestimates the outbreak diversity.

This work opens for more detailed investigations of predictability of epidemic processes. For example, our work assumes we know the starting point of the epidemic outbreak, which is fairly unrealistic. It would be interesting to investigate the situation with that situation relaxed. This would connect our line of research to the question of identifying the source of an outbreak [22–24] or reconstructing likely transmission trees [25, 26].

Acknowledgments

P.H. was supported by the Basic Science Research Program through the National Research Foundation of Korea (NRF) funded by the Ministry of Education (2013R1A1A2011947).

-
- [1] D. J. Sencer and J. D. Miller, *Emerg. Infect. Dis.* **12**, 29 (2006).
 - [2] D. Lazer, R. Kennedy, G. King, and A. Vespignani, *Science* **343**, 1203 (2014).
 - [3] J. Iwai and S. Sasa, e-print arXiv.org:1303.6606.
 - [4] S. Janson, M. Luczak, and P. Windridge, e-print arXiv:1308.5493.
 - [5] M. J. Keeling and K. Eames, *J. R. Soc. Interface* **2**, 295 (2005).
 - [6] M. Morris, ed., *Network Epidemiology: A Handbook for Survey Design and Data Collection* (Oxford, Oxford University Press, 2004).
 - [7] R. Pastor-Satorras, C. Castellano, P. van Mieghem, and A. Vespignani, e-print arXiv:1408.2701.
 - [8] J. O. Lloyd, S. J. Schreiber, P. E. Kopp, and W. M. Getz, *Nature* **438**, 355 (2005).
 - [9] M. Molloy and B. A. Reed, *Random Struct. Algorithms* **6**, 161 (1995).
 - [10] P. Holme, *Journal of Logistical Engineering University* **30**, 1 (2014).

- [11] S. Kininmonth, M. Drechsler, K. Johst, and H. P. Possingham, *Mar. Ecol. Prog. Ser.* **417**, 139 (2010).
- [12] D. J. Watts and S. H. Strogatz, *Nature* **393**, 440 (1998).
- [13] B. MacKay and N. Wormald, *J. Algorithm.* **11**, 52 (1990).
- [14] M. E. J. Newman, *Networks: An Introduction* (Oxford, Oxford University Press, 2010).
- [15] F. Liljeros, C. R. Edling, and L. A. N. Amaral, *Microbes Infect.* **5**, 189 (2003).
- [16] F. Liljeros, J. Giesecke, and P. Holme, *Mathematical Population Studies* **14**, 269 (2007).
- [17] G. Caldarelli, *Scale-Free Networks: Complex Webs in Nature and Technology* (Oxford, Oxford University Press, 2007).
- [18] R. Pastor-Satorras and A. Vespignani, *Phys. Rev. Lett.* **86**, 3200 (2001).
- [19] Y. Moreno, R. Pastor-Satorras, and A. Vespignani, *Eur. Phys. J. B* **26**, 521 (2002).
- [20] P. Holme, *PLoS ONE* **8**, e84429 (2013).
- [21] We use the Gauss-Newton non-linear least-squares method from the statistics software R <http://www.r-project.org/>.
- [22] A. Y. Lokhov, M. Mezard, H. Ohta, and L. Zdeborova, *Phys. Rev. E* **90**, 012810 (2014).
- [23] C. H. Comin and L. da Fontoura Costa, *Phys. Rev. E* **84**, 056105 (2011).
- [24] N. Antulov-Fantulin, A. Lancic, T. Smuc, H. Stefancic, and M. Sikic, e-print arXiv:1406.2909.
- [25] A. S. Walker, *et al.* *PLoS Med.* **9**, e1001172 (2012).
- [26] T. Jombart, A. Cori, X. Didelot, S. Cauchemez, C. Fraser, and N. Ferguson. *PLoS Comput. Biol.* **10**, e1003457 (2014).